“Venetian Blind” Direct Energy Conversion for Fusion Reactors

By Ralph W. Moir, William L. Barr, Lawrence Livermore Laboratory, University of California, Livermore, CA, United States of America

Contact information as of 2009 for Ralph Moir is Vallecitos Molten Salt Research, <RMoir@Pacbell.net>, 607 East Vallecitos Road, Livermore, CA 94550.

This work was performed under the auspices of the US Atomic Energy Commission.

Abstract

A new direct energy conversion technique that uses the angular-dependent transmission of ribbon grids, which resemble Venetian blinds, to recover the energy of particles leaking out of a fusion reactor is discussed. This converter works well, even to energies as low as 10 keV, because of its excellent space-charge handling ability. This low-energy operating range makes direct energy conversion possible on closed confinement devices; operation at about 100 keV might be useful on open confinement devices. Energy recovery efficiencies of 60 to 70% are predicted. Examples are presented in which a direct energy converter with efficiencies in this range, when viewed as a topping cycle to a thermal converter, could considerably improve the reactor prospects of both open- and closed-field-line confinement schemes.

1. Introduction

The principle of converting the kinetic energy of charged particles directly to electricity has been known for a long time. The first major application has been to recover the unused energy of electrons leaving a traveling wave tube.[1] The first seemingly practical application of recovering the energy of the plasma that leaks out of a fusion reactor is the work of Post.[2] His scheme has four main steps. First, the plasma is guided through a magnetic expander or nozzle that simultaneously reduces the density and converts the random motion to directed motion. Second, the electrons are separated from the ions. Third, the ions are slowed down by an electric field and separated into energy groups. Finally, the slow ions are collected on high-voltage electrodes, thus forming readily usable direct currents at high voltage. For energy separation, Post suggested using periodic electrostatic focusing, which guides the fast particles as they slow down. However, for sufficiently slow ions the focusing fails and the particles are diverted into a collector electrode.

The scheme we propose differs in that energy selection depends on the angular dependence of transmission through ribbon grids resembling a Venetian blind. We retain Post’s concept of the expander except that we expand in two dimensions instead of one. As is shown in Figure 1, the ions and electrons leak out of the confinement region via a divertor and are magnetically guided into the gridded structure. The magnetic field converts the random motion of the particles into a highly directed stream, at a slight angle from the normal to the plane containing the grids.

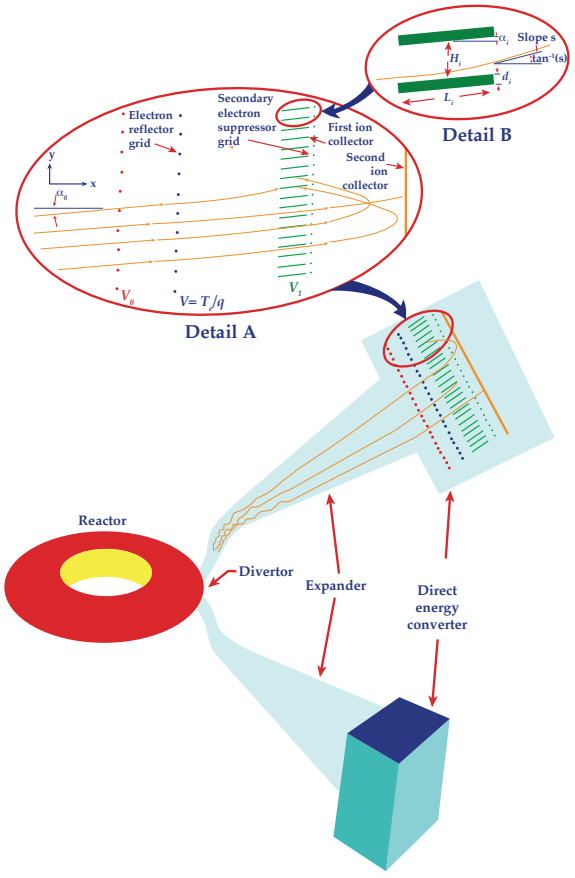

Figure 1 — “Venetian-blind” direct converter.

The function of the negative grid is to reflect the electrons and allow the ions to pass on toward the positive Venetian blind like ribbon grids. Initially the ions are directed at a slight angle to the applied uniform electric field. Therefore, the trajectories are parabolic, as is shown in Figure 1. A related idea, which also uses parabolic trajectories, is described by Richard Post.[3]

The incoming ion trajectories are aligned with the ribbons and thus see a rather tenuous grid. However, after the ions have lost their forward motion (in the x-direction) they turn around and see a rather opaque grid on their return path. The ions that hit the ribbon grid are collected and form a current at the voltage of that grid. The spacing between grids can be quite small (a few centimeters). Since the space-charge field is in the same direction as the applied field, space-charge effects are minimal, even at energy as as low as 10 keV. To handle large total powers, the area of the collector can be made large in both y- and z-directions, perpendicular to the directed motion. Since the grid spacings are small compared to the beam width, beam blow-up will not occur as a result of space charge.

2.0 Analysis of Collector Efficiency

Before writing the expressions for efficiency we need to calculate the particle's trajectory and transmission through the grids. The strength of the expander's magnetic field is so low at the collector that, although it penetrates the collector structure, its effects on trajectories in the collector should be negligible. From the conservation of energy we have:

$$\frac{1}{2}mv_y^2 = \frac{1}{2}mv_{y0}^2$$

and

$$\frac{1}{2}mv_x^2 + eV(x) = \frac{1}{2}mv_{x0}^2 \qquad (1a)$$

The slope of the particle at x is

$$S(x) = \frac{v_y}{v_x} = \frac{v_{y_0}}{\left(v_{x_0}^2 - \dfrac{2eV(x)}{m}\right)^{1/2}} \qquad (1b)$$

where the potential is V(x). Using the initial angle of the particle α_o and the initial energy W_o we obtain

$$\frac{1}{2}mv_{y_0}^2 = W_0 \sin^2\alpha_0$$

and

$$\frac{1}{2}mv_{x_0}^2 = W_0 \cos^2\alpha_0 \qquad \text{(Eq. 2)}$$

Then, we can rewrite S as follows:

$$S(x) = \frac{\sin\alpha_0}{\left(\cos^2\alpha_0 - \dfrac{eV(x)}{W_0}\right)^{1/2}} \qquad (3)$$

From Figure 1 we see that the transmission of the grids in the forward direction (T_f) is

$$T_{f_i} = 1 - \frac{L_i \sin\left|\tan^{-1}S_i - \alpha_i\right| + d_i \cos\left|\tan^{-1}S_i - \alpha_i\right|}{H_i \cos\left(\tan^{-1}S_i\right)} \qquad (4)$$

and in the backward direction is

$$T_{b_i} = 1 - \frac{L_i \sin\left|\tan^{-1}S_i + \alpha_i\right| + d_i \cos\left|\tan^{-1}S_i + \alpha_i\right|}{H_i \cos\left(\tan^{-1}S_i\right)} \qquad (5)$$

The subscript i refers to the i-th grid. The symbol L_i is the ribbon width, d_i the thickness, and H_i the ribbon spacing; α_i is the tilt angle of the ribbon. The expressions for transmission can be simplified, thus giving:

$$T_{f_i} = 1 - \frac{L_i}{H_i}\left|\sin\alpha_i - S_i\cos\alpha_i\right| - \frac{d_i}{H_i}\left(\cos\alpha_i + S_i\sin\alpha_i\right)$$

and

$$T_{b_i} = 1 - \frac{L_i}{H_i}\left|\sin\alpha_i + S_i\cos\alpha_i\right| - \frac{d_i}{H_i}\left(\cos\alpha_i - S_i\sin\alpha_i\right) \qquad (5b)$$

Space charge should not affect the efficiency because the slope of the trajectories, although slightly altered from the parabolic form, depends only on the local potential (see Equation 3), which is unaffected by space charge at the ribbons where the transmission is calculated.

The efficiency η is the fraction of the input power that is recovered:

$$\eta = \frac{\sum_i V_i x\left(\text{current collected on } V_i\right)}{\left(\text{input power}\right)} \qquad (6)$$

where V_i is the potential on the i-th grid. Let the current distribution dI/dW be given as a function of energy and be normalized so that the input power is unity:

$$\text{input power} = \int_0^\infty W\frac{dI}{dW}dW = 1 \qquad (6b)$$

For a one-stage device (N = 1), collector 1 is made opaque (T_f = 0). For two collectors (N = 2), collector 2 is made opaque and so on (Figure 2).

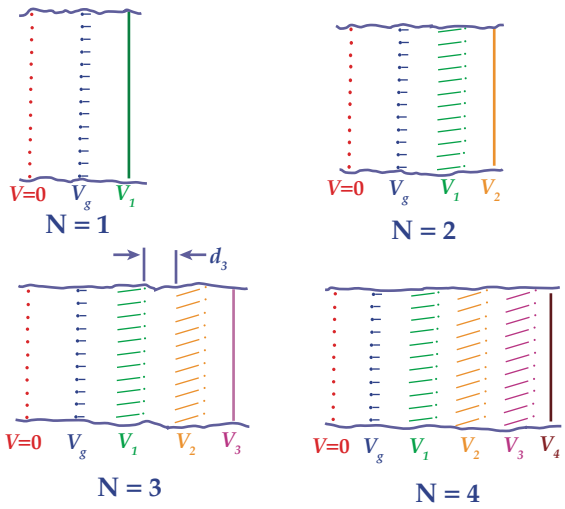

Figure 2 — Electrode configuration for the one-, two-, three-, and four collector devices.

It is interesting that for the one-collector device, the configuration and potentials are identical to a vacuum-tube triode. The efficiency of a single stage device can be written as:

$$N=1,\eta_1 = V_1\int_{V_1}^{\infty} T_{f_0}T_{f_g}\frac{dI}{dW}dW$$
$$-(1+\varepsilon)V_g\int_0^{\infty} T_{f_0}\left(1-T_{f_g}\right)\frac{dI}{dW}dW$$
$$-\left[\varepsilon\left(V_1-V_g\right)-V_g\right]\int_0^{V_i} T_{f_0}\left(1-T_{b_g}\right)\frac{dI}{dW}dW \qquad (6c)$$

where V_i' is equal to $qV_i/\cos^2\alpha_o$ and T_{f_0} and T_{f_g} are the transmissions of the grounded grid and the negative grid, respectively, and ε is the number of secondary electrons produced per ion hitting the grid. The first term gives the energy recovered from ions collected on V_1. The second term is negative and represents both the ions hitting the front of the electron reflector grid (V_g) and the secondary electrons leaving the grid. The last term represents the ions striking the back side of the electron reflector grid and the secondary electrons, which in this case stream to the collector (V_1).

For two collectors the efficiency is given as

$$\eta_2 = V_1\int_{V_1^*}^{V_2^*}\left[T_{f_0}T_{f_g}\left(1-T_{f_1}\right)+T_{f_0}T_{f_g}T_{f_1}\left(1-T_{b_1}\right)\right]\frac{dI}{dW}dW$$
$$+\int_{V_2^*}^{\infty}\left[V_1T_{f_0}T_{f_g}\left(1-T_{f_1}\right)+V_2T_{f_0}T_{f_g}T_{f_1}\right]\frac{dI}{dW}dW$$
$$-\int_{V_1^*}^{V_2^*}\left[\left(V_2-V_1\right)\varepsilon\left(1-T_{\text{grid wire}}\right)T_{f_0}T_{f_g}T_{f_1}-V_1\left(1-T_{\text{grid wire}}\right)T_{f_0}T_{f_g}T_{f_1}\right]\frac{dI}{dW}dW$$
$$-\left|V_g\right|(1+\varepsilon)\int_0^{\infty}T_{f_0}\left(1-T_{f_g}\right)\frac{dI}{dW}dW$$
$$-\left\{\varepsilon\left(V_1-V_g\right)\left(\frac{L_1}{H_1}\sin\alpha_1+\frac{d_1}{H_1}\cos\alpha_1\right)-V_g+\varepsilon\left(V_2-V_1\right)\left(\frac{L_1}{H_1}\sin\alpha_1-\frac{d_1}{H_1}\cos\alpha_1\right)\right\}$$
$$\text{x}\left[\int_0^{V_1^*}T_{f_0}T_{f_g}\left(1-T_{b_g}\right)\frac{dI}{dW}dW+\int_{V_1}^{V_2^*}T_{f_0}T_{f_g}T_{f_1}T_{b_1}\left(1-T_{b_g}\right)\frac{dI}{dW}dW\right] \qquad (6d)$$

The last term ([ ] [ ]) should be negligible because there are few particles below energy qV_1 and T_{b1} is near zero.

The expressions for three and four collectors are of the same form but have many more terms.

The terms that appear are of three basic types. Positive terms give the energy recovered from ions. Negative terms proportional to ε give the energy carried away by secondary electrons. The remaining negative term gives the energy lost as ion current to the negative grid. Any ions that are reflected and escape collection contribute nothing, as if they were collected at zero potential. They are, of course, included in η through the normalization of dI/dW.

Just behind each set of collector ribbons is the secondary electron suppression grid whose transmission is $T_{gridwire}$. We assume that the secondary electrons formed on the ribbon do not escape, but that each ion hitting the suppression grid creates ε secondary electrons which carry away considerable energy.

Two additional assumptions are made in the expression for collection efficiency. The first is that the equipotential surfaces are planar between grids. This is a good approximation, except near grid wires or ribbon edges where distortions will cause focus effects. The second is that there are no correlations from one grid to the next. This means, for example, that we neglect the effect of one grid creating a "shadow" on succeeding grids. Both of these effects should be analyzed further.

Two different current distributions were studied in detail: a "top hat" and an accelerated Maxwellian. These are shown in Figure 3 with a loss cone distribution[4] for comparison.

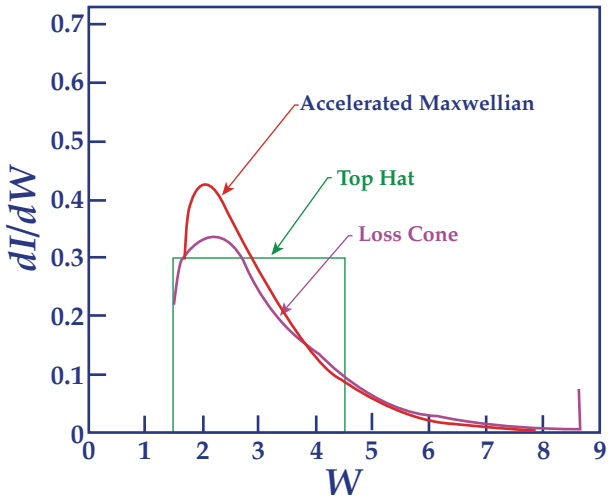

Figure 3 — Energy distribution of the ion current for three cases: loss cone appropriate to an open-end device, accelerated Maxwellian appropriate to a toroidal device, and a simple flat top distribution.

There are no ions having energy below some minima because we assume the plasma ambipolar potential is positive. This positive plasma potential accelerates ions and decelerates electrons. If the plasma potential were negative, the current distribution would extend down to zero energy.

The procedure used to find the optimum efficiency was to choose the entrance angle α_o and then vary each parameter, such as the ribbon dimensions, angles, and spacings, by a small amount so that the efficiency increased. Once the optimum efficiency was found, the angle α_o was varied to find the best angle. The values of T_{fo}, T_{fg}, and T_{bg} were 0.99. The potential of the negative grid V_g was always taken to be -0.2 times the minimum energy or approximately 10% of the mean energy. The results of this optimization technique for the two distributions are given in Tables 1 and 2.

To see the effect of finite ribbon width on efficiency, all of the parameters except d/L_i were held constant. Then, the efficiency for various values of d/L_i was calculated. These results are shown in Figure 4a. Figure 4b shows the effect of varying the entrance angle, α_o. In a real situation the entrance angle would have a spread, perhaps ±0.03 radians. Figure 4c is a plot of efficiency versus number of collectors showing each of these effects.

We see that the top hat distribution, which had a narrower energy spread, gave a higher efficiency than the accelerated Maxwellian. This suggests a way of improving the efficiency: separate the input beam into groups, each having a smaller spread. From Figure 4 we see that the top hat distribution, including angular spread, finite ribbon width, and secondary electrons, gave efficiencies of 55, 67, 72, and 75% for one, two, three, and four collectors. In all cases the loss of efficiencies as a result of secondary electrons was less than 1%, with $T_{gridwire}$ = 99%, and $\varepsilon = 3$.

The overall direct energy conversion efficiency will include losses other than in the collectors (e.g. charge exchange and beam interception by support structures). However, it is hoped that the overall efficiency will be close to the collection efficiency.

Table 1 — Optimum Parameters for the "Top Hat" Distribution

N	α_0	α_1	α_2	α_3	L_1/H_1	L_2/H_2	L_3/H_3	η	η_{sec}
1	0	—	—	—	—	—	—	0.547	-0.009
2	0.169	0.169	—	—	2.448	—	—	0.688	-0.008
3	0.188	0.188	0.236	—	2.05	1.803	—	0.753	-0.008
4	0.195	0.195	0.23	0.288	1.809	1.612	1.505	0.777	-0.007

Table 2 — Optimum Parameters for the Accelerated Maxwellian Distribution

N	α_0	α_1	α_2	α_3	L_1/H_1	L_2/H_2	L_3/H_3	η	η_{sec}
1	0	—	—	—	—	—	—	0.531	-0.006
2	0.12	0.16	—	—	2.545	—	—	0.66	-0.007
3	0.14	0.183	0.21	—	2.063	1.976	—	0.709	-0.008
4	0.16	0.213	0.23	0.257	1.691	1.582	1.612	0.735	-0.008

Experiments described elsewhere[5] were performed on the one-collector configuration. A hydrogen plasma from a pulsed plasma source was directed at the one-collector device, and the collector potential was varied to experimentally find the optimum efficiency giving the results shown in Figure 5. The computed efficiency was based on a measured energy distribution that was very wide (100 to 1500 eV) and varied considerably from shot to shot. As a result of this variation, the experimental efficiency data have considerable scatter except near the peak where agreement between theory and experiment was good and gave an efficiency of 40%.

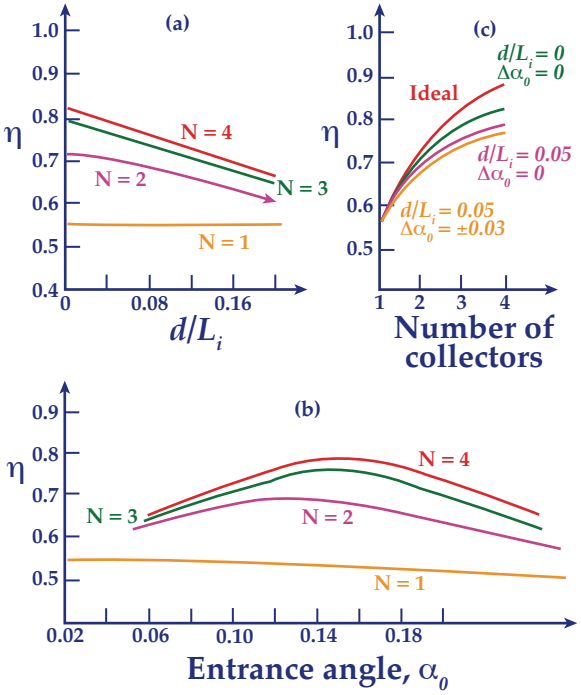

Figure 4 — Parametric dependence of efficiency: (a) variation of ribbon thickness, (b) variation of entrance angle, and (c) variation of number of collectors.

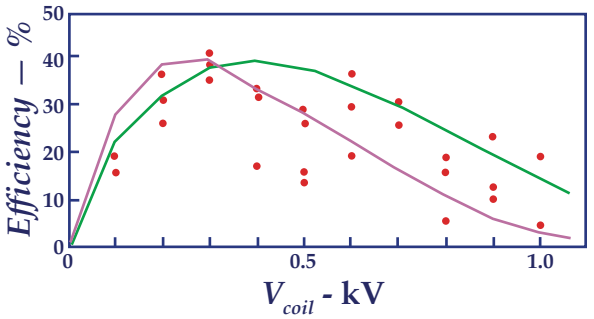

Figure 5 — Efficiency versus collector voltage for the one-collector device. The dots are experimental data and the solid curves are theoretical efficiencies using two different but typical ion-energy distributions.

3 Power Flux Limit: Space-Charge and Heating

The maximum power flux that can be handled is determined by thermionic emission from the heating of grid wires by beam interception. The maximum current density on the other hand is set by space charge. The grid spacing can be adjusted so that the power flux and the current density are simultaneously maximized.

3.1 Space-Charge Limit

Consider a one-dimensional system for direct recovery with collectors at potentials V_j located at $x = x_j$. Assume that particles with energy W greater than qv_j pass through the range $x < x_j$ and do not return, Particles with energy less than qV_{j-1} never reach $x = x_{j-1}$. Then, for $x_{j-1} < x \le x_j$ the potential is $V = V(x)$ and the charge density is:

$$qn(x) = \sqrt{\frac{M}{2}} - 2\int_{qV(x)}^{qV_j} \frac{(dJ/dW)dW}{\sqrt{W - qV(x)}} + \int_{qV_j}^{\infty} \frac{(dJ/dW)dW}{\sqrt{W - qV(x)}}, x_{j-1} < x \le x_j \qquad (7)$$

where dJ / dW is the energy distribution of the current density, and the first term includes the reflected particles. The potential is determined from Poisson's equation:

$$\frac{d^2y}{dx^2} = -\frac{qn(x)}{\varepsilon_0} \quad (8)$$

Boundary conditions for space- charge-limited current are:

$$V(x_j) = V_j, \left(\frac{dV}{dx}\right)_{x_j} = 0$$

and

$$V(x_{j-1}) = V_{j-1} \quad (9)$$

Therefore, the magnitude of the total current density:

$$J = \int_0^\infty \frac{dJ}{dW} dW$$

which is limited by space charge between the j-1-th and j-th electrode is determined for any distribution dJ/dW. If there are N collector's there will, in general, be N different limiting values of J. The collector design can be optimized by varying the spacing:

$$\ell_j = x_j - x_{j-1}$$

to make all cells space-charge limited simultaneously. These are the maximum allowed values. In practice one might prefer to make all ℓ_j equal to the smallest calculated one.

If we call J_j the value of J that results in zero potential gradient at the j-th electrode, it can be shown that:

$$J_j = A(V_j - V_{j-1})^{3/2} \ell_j^{-2}, j > 1$$
$$J_1 = A(V_1 - V_g)^{3/2} \ell_1^{-2} \quad (10)$$

which is the familiar form for space-charge limited current. Here, however, the coefficient A depends on the distribution function and on N.

A computer program was written to solve by iteration the N values of l_j for any specified energy distribution and total current density. The N values of collector potential V_j are determined by a separate iterative calculation that gives the optimum values for the particular energy distribution.

As an example, a calculation was made for a displaced Maxwellian distribution of ions, as shown in Figure 3. The results are given in Table 3 for N = 1, 2, 3, 4, and 5 collector stages. Input current density was chosen to give P = 100 W/cm² for one case with a mean energy of 30 keV and another with a mean energy of 150 keV. In these two cases, it was possible to have small enough spacings so that space charge did not limit the power flux but rather the power flux was limited to 100 W/cm² by grid heating, as will be discussed later. Reasonable grid spacings are found for energies down to and below 10 keV.

For comparison of space-charge handling, consider a 22-stage periodic focusing direct energy converter.[2] The space-charge-limited power was calculated[6] to be 300 W / cm² for a beam height of 1 m and a mean energy of 800 keV. Since it is expected that the beam height could scale as $W^{1/2}$, we would expect:

$$P / A \propto W^{5/2} / \ell^2 \propto W^{3/2}$$

Then 100 W/cm² would be achievable for a mean energy of 385 keV, at 150 keV the space-charge limited power flux would be down to 24 W/cm², and at 30 keV the power would be only 2 W/cm².

We see that the Venetian-blind direct energy converter can handle considerably more power flux than the periodic-focus converter for energies below 300 keV. This is because, in the Venetian blind converter, the space- charge electric field is collinear with the applied field and particle trajectories and thus can be large, whereas, in the periodic focusing converter, the space-charge electric fields are transverse to the applied field so that relatively small amounts of space charge will upset the focusing properties.

These space-charge considerations mean that the periodic focusing system is best suited for high energies and, hence, open-end confinement. The Venetian-blind system may be most useful for low-energy, closed containment. In addition, it has the possibility of also being used for open-end containment systems.

Table 3 — Parameters for Space-Charge-Limited Conditions for an Accelerated Maxwellian Distribution

N	j	W = 30 keV J = 3.33 mA / cm²		W = 150 keV J = 0.67 mA / cm²	
		V_j (kV)	ℓ_j (kV)	V_j (kV)	ℓ_j (kV)
1	1	18.6	27.8	93	208
2	1	16	29.7	80	222
	2	28.8	27	144	202
3	1	15.4	30.7	77	230
	2	23.8	19.8	119	148
	3	35.8	34	179	254
4	1	15.4	30.7	77	230
	2	21.8	16.8	109	126
	3	29.6	22.9	148	171
	4	41	41	205	306
5	1	15.2	31	76	232
	2	20.4	15	102	112
	3	26.2	18.1	131	135
	4	33.6	25.9	168	194
	5	45	48.5	225	363

3.2 Electrode Heating Limit

That part of the incoming power not directly recovered will appear as heat on the various surfaces that are bombarded. This heat can be conducted from the more massive electrodes, but will have to be radiated from the rather fine grid wires. Thus, higher power flux will mean hotter grids. Since the grids must not get hot enough to emit too many thermionic electrons, the power flux is limited. We can determine the limiting power flux by calculating the temperature and the resulting emission current as function of power flux.

The power radiated from a tungsten grid wire is:

$$P_r = \sigma \varepsilon T^4 \qquad (11)$$

where $\sigma = 5.7 \times 10^{-12}$ W/cm² deg⁴, the emissivity $\varepsilon \approx 0.23$ for tungsten at $T = 1500$°C. At equilibrium, $P_r A_r = P_b A_b$, where P_b is the incident power flux, and A_r and A_b are the total radiating area and bombarded area, respectively. For round wires $A_r = \pi A_b$. Solving for temperature gives:

$$T = \left(\frac{P_b A_b}{A_r \sigma \varepsilon} \right)^{1/4} \qquad (11b)$$

Thermionic emission current at temperature T is given by the Richardson-Dushman equation:

$$J_e = CT^2 \exp(-e\phi / kT) \quad (12)$$

where C = 72 A/cm² and work function ϕ = 4.52 V for tungsten.

Emission current can probably be tolerated to a current density where, on the average, one electron is emitted for each ion that strikes the grid. This criteria can be stated as follows: With a 99% transmitting grid this one ion would constitute about a 1% loss in efficiency and the electron a fraction of 1%, since it will usually be caught on the nearest positive electrode. Therefore, we put:

$$J_e A_r = J_b A_b \quad (12a)$$

where $J_b = P_b\, e/\overline{W}$ is the ion-current density for ions of mean energy $\overline{W}$. Thus, the maximum allowable power flux is

$$P_b = \frac{\bar{W} J_b}{e} = \frac{\bar{W} J_e A_r}{e A_b} \quad (13)$$

or

$$\left(\frac{A_b P_b}{A_r}\right)\left(\frac{e}{\bar{W}}\right) = J_e \quad (14)$$

But, $A_b P_b / A_r = P_r$, therefore the limiting condition is

$$\frac{P_r}{\bar{W}/e} = J_e \quad (14b)$$

By using Equations (11) and (12) we can express J_e as a function of P_r, so that this relationship determines the maximum P_r and hence P_b for any mean energy $\overline{W}$ of the incident ions. Figure 6 shows a plot of $P_{b(max)}$ versus $\overline{W}$ for two different ratios of A_r/A_b. Round wires have an area ratio of π; a ribbon may have an area ratio of 20 or more. To keep thermionic current less than intercepted beam current, the beam power must fall below the line in Figure 6. This implies that the power level must be kept below about 50 W/cm² for round wires or 300 W/cm² for a ribbon having an area ratio of 20. To allow for possible misalignment of the ribbons, 100 W/cm² is a reasonable upper limit. At these power levels, the grids will run rather hot (~1900 °K) thus, the possible metals that the grids could be made from are limited. Tantalum and molybdenum have lower work function than tungsten and, therefore, emit more thermionic electrons. Rhenium would be better than tungsten. Nickel and platinum melt at too low a temperature.

To avoid electrical breakdown, the voltage gradients will have to be kept below some critical value and current limiters will be required to avoid damage to the delicate grid structure from sparking. Problems such as component life-time, pumping, and heat transfer will be left for future work.

Some experimental evidence[7] exists which indicates that these power levels are tolerable. One kilowatt of 20 keV protons impinged on tungsten ribbons (2 mils x 45 mils) with no apparent ill effects after 1 hour of operation. The beam area was 6.5 cm² giving about 200 W/ cm². The voltage difference between one set of grids and the next was 20 kV.

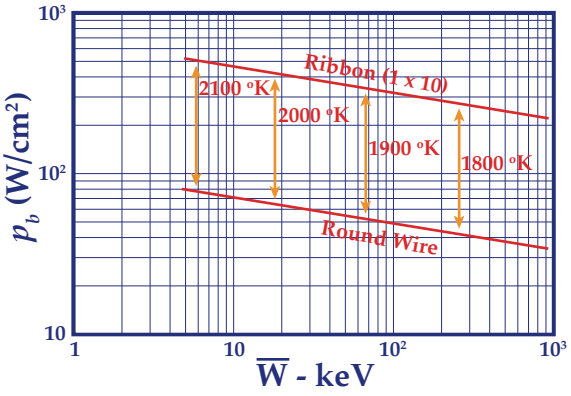

Figure 6 — Thermionic limited incident power flux versus mean energy. Grid wire temperatures are indicated.

4. Expander

The expander is a multi-purpose component of the direct converter. It guides the plasma from the confinement region, transforms the random motion into a very directed beam, serves to reduce the power flux (power per unit area), and transfers virtually all of the energy in the electrons to the ions via the ambipolar potential. Let us consider these functions individually.

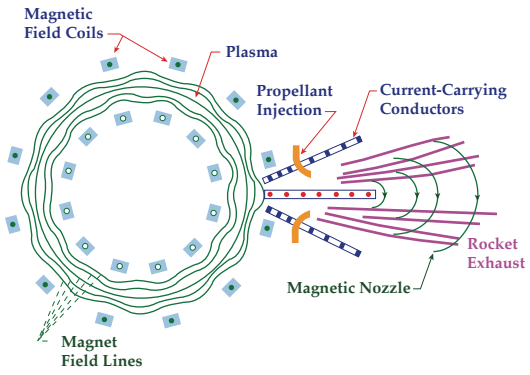

Figure 7 — Toroidal fusion reactor with a diverter and expander used for a rocket
(by courtesy of J.R. Roth; NASA. Lewis)

The plasma particles will eventually escape the confinement region and leak out through specially designed divertors. Figure 7 shows an example[8] of such a divertor. The magnetic field lines of the divertor define the beginning of the expander entrance. The plasma can be guided (around corners if desired to avoid neutron leakage) from the reactor. The magnetic field strength of the expander drops by a large factor (~1000) as it guides the plasma into the collector. If the rate of change of the field strength is sufficiently small, the trajectories will behave adiabatically. That is, the particle guiding centers will approximately follow the field lines, and the energy perpendicular to the magnetic field $W_\perp$ will be

$$W_\perp = W_{\perp M}\frac{B}{B_M} \quad (15)$$

where $W_{\perp M}$ is the perpendicular energy and B_M is the magnetic field at the expander entrance. The angle α that the particle's velocity vector makes with respect to the field lines is

$$\sin\alpha = \sqrt{\frac{W_\perp}{W}} = \sqrt{\frac{W_{\perp M}}{W}}\sqrt{\frac{B}{B_M}} \quad (16)$$

The ratio of magnetic field at the entrance and exit of the expander is denoted as R. For R = 1000, α is less than 0.033 since, $(W_{\perp M}/W)^{0.5} \leq 1$. This constitutes a highly directed beam.

For conservation of magnetic flux,

$$\phi = \int \vec{B}\cdot\vec{\eta}\,dA \quad (16b)$$

we see that the cross-sectional area of the beam increases from A divertor to A collector by a factor of R:

$$A_{collector} = RA_{divertor} \quad (16c)$$

It then follows that the power flux

$$(P/A)_{collector} = (1/R)(P/A)_{diverter} \quad (17)$$

As we have already seen, from the standpoint of space charge and heating as a result of the beam intercepting metal surfaces, it is necessary to reduce the power flux to about 100 W/cm^2.

The last function is the energy transfer from electrons to ions. The random motion of the electrons is converted to motion directed along the field lines. If the electrons have an appreciable energy as they enter the expander, their velocity will greatly exceed the ion velocity. Since the ion density is dropping roughly proportional to B and approximate charge neutrality is required (because the Debye length is short), the electrons will be prevented from running away from the ions by an (ambipolar) electric field set up by a small charge density imbalance.

This phenomenon is the same as that giving rise to the electrostatic confinement of electrons in a magnetic mirror. The resulting ambipolar potential drop will adjust itself in a self-consistent manner so that the mean electron velocity and current at the collector will equal that of the ions. Thus, the electron energy will be on the order of m_e/m_i smaller than the ion energy, i.e. negligible.

The main difference between this expander and that of Post's [2] is that here expansion can be two-dimensional (conical shaped) rather than one-dimensional (fan shaped). Thus the area can increase as r^2 rather than r so that a much larger collector area can be achieved, and perhaps the expander can be smaller than the fan-shaped expander.

For example, modules having surface areas 10 meters by 10 meters could handle 100 MW. Considerable cost reduction might result from these rather small unit sizes compared to Post's fan-shaped expander. Another possibility for the expander is to have the field drop off so suddenly that the particles essentially follow straight lines, as if emerging from a point source. The collector structures would lie on spherical surfaces with the point source somewhat off centre so that the ions would enter the collector structure at an angle α_o from the normal.

5. Topping Cycle Considerations

As the previous analysis indicated, this technique for direct conversion has a rather modest efficiency, perhaps 60 to 70%. One wonders just how high the efficiency must be to make its application on a fusion reactor interesting. With the objective of determining the required collection efficiency we now discuss the overall efficiency of a fusion reactor.

One can look on this or any direct converter as a topping cycle to a thermal system which itself could have a topping cycle. In the power system shown in Figure 8, the fusion reactor is characterized by nuclear power generated/injected power, Q; the fraction of fusion energy released in the form of charged particles, f_c; and the fraction of non-charged (mostly neutrons) energy released, f_n.

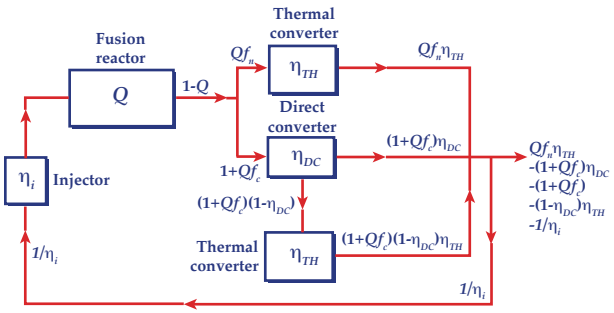

Figure 8 — Power-flow chart

Any energy lost from charged particles by radiation or charge exchange will be lumped into f_n.

Next, we must decide on a figure of merit for the system. The conventional figure of merit is overall capital cost and operational cost. To avoid estimating component costs, we use the ratio of power into a particular component to the net electrical power output as our figure of merit. There are four large components: injector, magnet, direct converter, and thermal converter. One of the most expensive items might be the thermal converter, therefore, we define the figure of merit as G, where G = power into the thermal converter / net electrical power. The expression for G can be written by inspection of Figure 8 as

$$G = \frac{Qf_n + (1+Qf_c)(1-\eta_{DC})}{Qf_n\eta_{TH} + (1+Qf_c)\eta_{DC} + (1+Qf_c)(1-\eta_{DC})\eta_{TH} - 1/\eta_i} \tag{18}$$

which after simplification becomes (since $f_c + f_n = 1$):

$$G = \frac{1 - f_c\eta_{DC} + \dfrac{1-\eta_{DC}}{Q}}{\eta_{TH} + f_c\eta_{DC}(1-\eta_{TH}) + \dfrac{\eta_{TH}(1-\eta_{DC}) + \eta_{DC} - 1/\eta_i}{Q}} \tag{19}$$

Now evaluating G(Q = ∞) for the case of no charged products (f_c = 0) gives:

$$G(Q=\infty, f_c = 0) = 1/\eta_{TH} \tag{19b}$$

This case corresponds to a fossil fuel or a fission power plant where the recirculated power is negligible. We will now look at the ratio of G to G (Q = ∞, f_c = 0), which compares the size of thermal conversion equipment needed in the fusion system under study to that required in a conventional power plant to achieve the same electrical power output. This is a good figure-of-merit parameter because it indicates the effect of recirculated power:

$$\frac{G}{G(Q=\infty, f_c=0)} = \frac{1 - f_c\eta_{DC} + \dfrac{1-\eta_{DC}}{Q}}{1 + f_c\eta_{DC}\dfrac{(1-\eta_{TH})}{\eta_{TH}} + \dfrac{1-\eta_{DC} + \dfrac{\eta_{DC}}{\eta_{TH}} - \dfrac{1}{\eta_i\eta_{TH}}}{Q}} \tag{20}$$

Another useful figure of merit is the overall plant efficiency, $\eta_{overall}$ defined as the ratio of output electrical power to power produced:

$$\eta_{overall} = \eta_{TH} f_n + \eta_{DC} f_c + f_c(1-\eta_{DC})\eta_{TH} + \frac{\eta_{DC} + (1-\eta_{DC})\eta_{TH} - 1/\eta_i}{Q} \tag{20b}$$

We will take η_{TH} = 0.45 and η_i = 0.90 for our examples. Modern power-plants have a thermal efficiency close to 40% but future improvements in materials will surely raise that figure. Injector efficiency of 90% is probably achievable by using a simple direct recovery system to recover any unused beam. We will consider first the D-T fuel cycle. Each fusion reaction releases a 3.5 MeV ^{4}He and a 14.06 MeV neutron. The neutrons will release more energy through exothermic reactions in the blanket. These reactions are

$$Li^6(n,\alpha)\,T + 4.78\ MeV$$

Bremsstrahlung and synchrotron radiation will effectively reduce the 3.5 MeV of charged energy. For our example we arbitrarily assume that 5% of the charged energy will be converted to thermal energy, thus we take f_c = (3.5 - 0.05 x 3.5) MeV / 22 MeV and f_n = 1 - f_c.

The results from Equations (20) and (21) are shown in Figures 9 and 10 for a range of values of η_{DC} and Q. The curve for G/G(Q = ∞, f_c = 0) = 1.0 is interesting; it shows the Q and η_{DC} values needed so that the recirculated power is handled entirely by the direct conversion equipment, and the values needed for the net electrical power coming entirely from the thermal conversion equipment. Recent calculations[9] of Q for D-T mirror machines range from 1 to 2. With a 70% direct conversion efficiency, which might be achievable with the Venetian blind / direct conversion technique, the thermal conversion capacity would range from 3% to 25% more than for a conventional power plant. Since 25% excess thermal capacity might be economical, we conclude that the Venetian-blind direct-converter might be useful if Q approaches 2, even though the efficiency is only 70%.

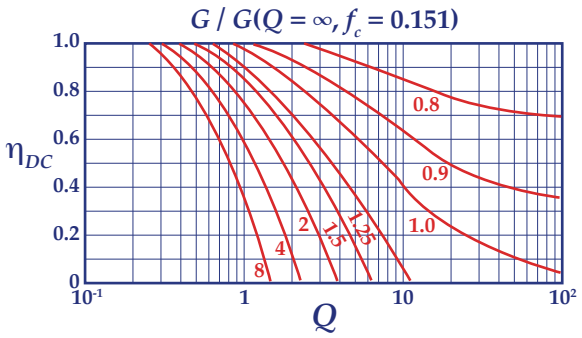

Figure 9 — Ratio of thermal conversion equipment required for the D-T reactor to that required on a conventional steam plant for the same electrical power output with η_{DC} and Q as independent parameters ($f_c = 0.151$)

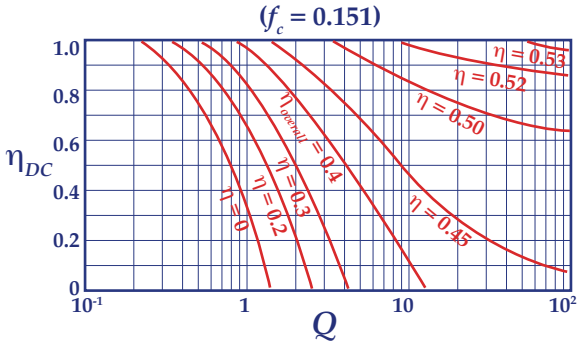

Figure 10 — Overall thermal conversion efficiency for the D-T reactor ($f_c = 0.151$)

For very high Q values, the reactor is essentially self-sustaining and corresponds to the closed confinement situation. For example, with Q = 100 the overall efficiency is increased from 45 to 50% and the thermal capacity needed is reduced by 20% for a direct conversion efficiency of 70%.

To reduce the circulating power, one might consider using the extra neutrons to produce fissioning either directly in the blanket or, as Lidsky[10] suggests, to capture the neutron in fertile material (^{238}U or thorium) to produce fissile material that is fissioned in a separate reactor.

In either case, the fission energy directly or indirectly increases the energy per fusion reaction. To evaluate the favorable effect on the power balance from fission we have evaluated Equations (20) and (21) using 100 MeV as the energy released per fusion event. The resulting value of f_c is 0.03325; the corresponding Q values are approximately 5 times the usual values. These results are shown in Figures 11 and 12. Note that for Q from 5 to 10 (corresponding to 1 to 2 without fission) the excess thermal capacity is considerably less than 25%, even for a direct conversion efficiency as low as 50%.

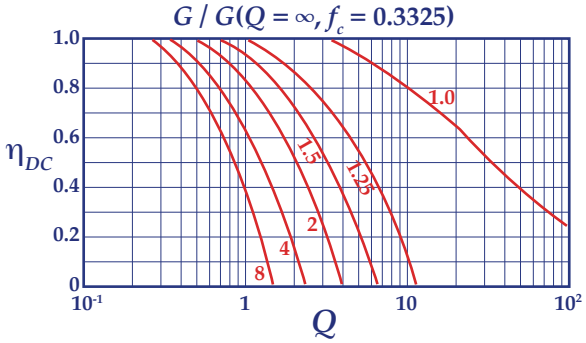

Figure 11 — Ratio of thermal conversion equipment required for the D-T reactor with fission to that required on a conventional steam plant for the same electrical power output ($f_c = 0.03325$)

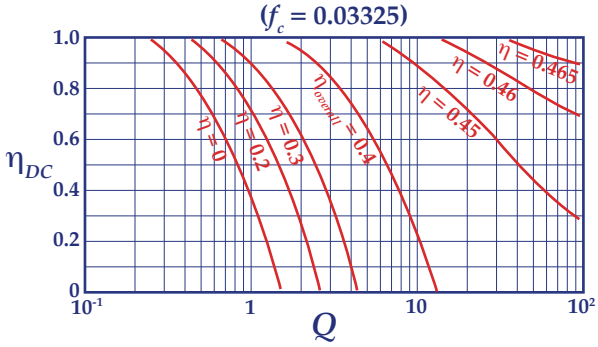

Figure 12 — Overall thermal conversion efficiency for the D-T reactor with fission ($f_c = 0.03325$)

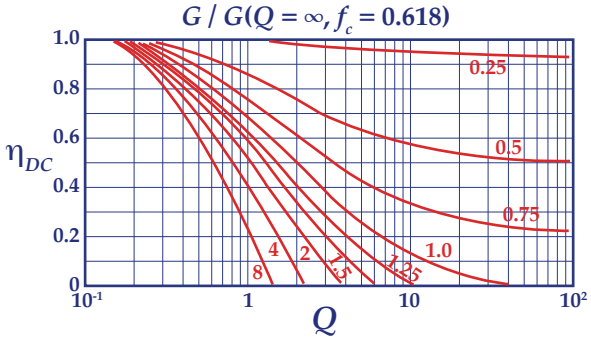

Figure 13 — Ratio of thermal conversion equipment required for D-D burn reactor to that required on a conventional steam plant for the same electrical power output ($f_c = 0.618$)

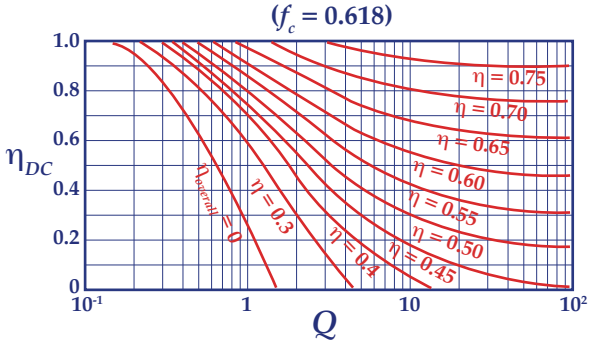

Figure 14 — Overall thermal conversion efficiency for the D-D burn reactor (f_c = 0.618)

As a final example, consider the D-D-T-^{3}He reaction where we assume no external breeding and all T and ^{3}He from the D-D reactions eventually fuse. The net reactions can be written as follows:

6 D → 2 ^{4}He + 2p
+ n(2.45 MeV)
+ n (14.06 MeV)
+ 26.72 MeV charged
+ 16.51 MeV neutrons

The fraction of charged fusion energy released f_c is 0.618. Results of the evaluation of Equations (20) and (21) for this complete D-D burn case are plotted in Figures 13 and 14. For a toroidal reactor (Q = 100) with η_{DC} of 60%, the overall efficiency would be 65% with only half the thermal conversion capacity needed by a system without direct conversion.

Conclusions

A new direct energy conversion technique that is quite simple in principle has been presented: The particles follow parabolic paths in a uniform electric field. Our analysis indicates efficiencies of 60 to 70%, depending on various conditions.

The device can operate down to very low energies (10 keV) in spite of space charge because the space charge fields can be comparable to the applied fields (they are parallel), and electrode spacings can be made small. The low-energy feature of this direct energy conversion concept should allow its use on toroidal confinement devices thus improving their conversion efficiency. Operation around 100 to 200 keV might be practical on open-end confinement devices.

Acknowledgements

We should like to thank Tom N. Haratani for assistance with the numerical calculations and Richard F. Post and T. Kenneth Fowler for support of this research.

For further information, William L. Barr, et al., "A Preliminary Engineering Design of a Venetian Blind Direct Energy Converter for Fusion Reactors," IEEE Transactions of Plasma Science PS-2, 71 (1974).

Publishing History

Manuscript received 21 August 1972; first published January 1973.

Reformatted and color illustrations provided January 2009 by Mark Duncan.

References

[1] Takanori Okoshi; E. Chin; S. Matsuki; "The tilted electric field soft-landing collector and its application to a traveling-wave tube," IEEE Transactions Electron Devices 19 (January 1972). For references to earlier work in this field see the references in this article, pp. 104-110

[2] Richard F. Post; Proceedings British Nuclear Energy Society Conference Nuclear Fusion Reactors (Culham Laboratory, Culham, England, 1969), UKAEA (1970) 88-111.

[3] William L. Barr; Lawrence Livermore Laboratory, Report UCRL-51147 (1971); O.A. Vinogradova, et al.; Atomic Energy 331 (1972) 586.

[4] The energy distribution of particles leaking to a mirror machine was calculated by A. H. Futch and refined by L. S. Hall using the Fokker-Planck computer code of Reference [9].

[5] Controlled Thermonuclear Research Annual Report, Lawrence Livermore Laboratory, Report UCRL-50002-70 (1970) 2-37 to 2-42.

[6] Ralph W. Moir; William L. Barr; Robert P. Freis; Richard F. Post; in Plasma Physics and Controlled Nuclear Fusion Research (Proceedings Conference Madison, Wisconsin, 1971) 3, IAEA, Vienna (1971) 315.

[7] Ralph W. Moir; Wiliam L Barr; Gordon W. Hamilton; John E. Osher; Bulletin American Physics Society 15 (1970) 1431.

[8] R. Roth; W. Rayle; I. Reinmann; New Scientist 54 (1972) 125.

[9] Artcher H. Futch Jr.; John P. Holdren; John Killeen; Art A. Mirin; "Multi-species Fokker-Planck calculations for D-T and D-^{3}He mirror reactors," Plasma Physics 14 (1972) 211

[10] Lawrence M. Lidsky; Proceedings British Nuclear Energy Society Conference Nuclear Fusion Reactors (Culham Laboratory, Culham, 1969), UKAEA (1970) 41-53.